Journal of Physiology (1988), **401**, *pp.* 567–579
With 6 text-figures
Printed in Great Britain

QUANTAL SECRETION AT RELEASE SITES OF NERVE TERMINALS IN TOAD (*BUFO MARINUS*) MUSCLE DURING FORMATION OF TOPOGRAPHICAL MAPS

BY MAX R. BENNETT AND NICKOLAS A. LAVIDIS
From the Neurobiology Research Centre, University of Sydney, N.S.W. 2006, Australia

(*Received 27 October 1987*)

SUMMARY

1. The number of quanta secreted from selected sites along terminal branches at suppressed synapses in the developing toad (*Bufo marinus*) gluteus muscle has been determined. The topographical projection from segmental nerves 8 and 9 to the ventral surface of this muscle matures slowly as toads develop in size from 12 to 40 g. Terminal branches of nerves 8 and 9 were visualized by prior staining with the fluorescent dye, 3-3-diethyloxardicarbocyanine iodide ($DiOC_2(5)$).

2. The evoked quantal release recorded with an extracellular electrode ($\bar{m}_e$) at different positions along the length of terminal branches at synaptic sites innervated either by nerve 8 ($\bar{m}_{e,8}$) or nerve 9 ($\bar{m}_{e,9}$) was determined in an external Ca^{2+} concentration, $[Ca^{2+}]_o$, of 0·35–0·45 mM. For over 90% of branches longer than 80 μm, $\bar{m}_e$ declined along exponential curves from a relatively large value at the proximal end of branches for both nerve 8 and nerve 9 terminals; the exponent for these exponential curves gave quantal length constants that varied from 26 to 80 μm (48 ± 4 μm, mean ± S.E.M.) depending on the length of the branch.

3. The evoked quantal release recorded with an intracellular electrode ($\bar{m}$) at synaptic sites dually innervated by nerve 8 and nerve 9 was nearly always (> 90%) greater for nerve 8 terminals than for nerve 9 terminals. At singly innervated sites the value of $\bar{m}$ per 100 μm length of terminal declined approximately exponentially with an increase in total terminal length (length constant 400 μm). However, at dually innervated sites the value of $\bar{m}$ per 100 μm length of nerve 9 terminal was very low at all total terminal lengths compared with singly innervated sites; this indicates that nerve 9 terminals were suppressed at dually innervated sites.

4. At five dually innervated sites, seven out of nine terminal branches of nerve 8 showed an exponential decline in $\bar{m}_{e,8}$ along their length, from a relatively large value near the proximal end of the branches (length constant 35 ± 3 μm, mean ± S.E.M.). In contrast, all the terminal branches of nerve 9 greater than 80 μm showed a uniformly low value of $\bar{m}_{e,9}$ along their length.

5. It is suggested that the suppression of nerve 9 terminals at dually innervated sites is primarily due to a decrease in the probability of secretion of normally highly secreting release sites at the proximal end of terminal branches.

INTRODUCTION

Amphibian muscles receive a topographical innervation from their motoneurone pools (Sherrington, 1892; Bennett & Lavidis, 1982*a*). Each of the segmental nerves subserving a motoneurone pool preferentially innervates a restricted part of a muscle. However, this is not the case during development when amphibian muscle fibres receive an extensive polyneuronal innervation (Bennett & Pettigrew, 1975; Letinsky & Morrison-Graham, 1980; Morrison-Graham, 1983). Many of the synaptic sites are innervated by several segmental motor axons (Bennett & Lavidis, 1982*a*, 1986) and the mature segmental pattern of innervation emerges with a gradual decrease in polyneuronal innervation. At synaptic sites which receive a dual innervation from two segmental nerves, one usually shows a lower efficacy of quantal transmitter release than the other (Malik & Bennett, 1987). The basis of these differences in secretion from the terminals of different segmental nerves during the establishment of topographical maps is unknown.

Amphibian motor-nerve terminals consist of hundreds of release sites or active zones from which quanta of transmitter may be released (Couteaux & Pecot-Dechavassine, 1968; McMahan, Spitzer & Peper, 1972; Dreyer, Peper, Akert, Sandri & Moore, 1973; Miller & Heuser, 1984). The probability of quantal secrtion from the release sites on arrival of the nerve impulse is not uniform: some release sites have a probability of secretion which is smaller than others (Bennett & Lavidis, 1979; Zefirov & Stolov, 1981; D'Alonzo & Grinnell, 1985; for a review see Robitaille & Tremblay, 1987). The spatial distribution of the release sites with different probabilities is such that sites closest to the origin of terminal branches tend to have higher probabilities for secretion than those that are more distal (Bennett & Lavidis, 1982*b*). However, this relationship does not hold for all terminal branches. Branches less than 80 μm in length generally show a uniformly low probability for secretion along their length, whereas nearly all branches longer than 80 μm show an approximately exponential decline from a high value near the origin of the branch (Bennett, Jones & Lavidis, 1986). In the present work a description is given of the probability of secretion along the terminal branches at synaptic sites dually innervated by different segmental nerves during the period of refinement of topographical maps. It is shown that the reduced secretion at terminals with low quantal efficacy is associated with a decrease in the amount of secretion at proximal release sites along terminal branches.

METHODS

Toads (*Bufo marinus*) weighing between 15 and 62 g were anaesthetized by immersion in 0·1% tricaine methanesulphonate (MS-222; Rural Chemical Industries, Australia) and then killed by cervical fracture. The gluteus magnus muscle with attached segmental nerves 7, 8, 9 and 10 was dissected free from surrounding connective tissues and placed in a Perspex organ bath of 3 ml capacity. The muscle was pinned on Sylgard with the ventral surface up and stretched to approximately 110% of its resting length in the limb. The bath was perfused at room temperature (16 ± 2 °C) with a modified Ringer solution of the following composition (mM): Na^+, 117; K^+, 3·0; Mg^{2+}, 2·0; Cl^-, 104·1; $H_2PO_4^-$, 0·64; HPO_4^{2-}, 9·7; Ca^{2+}, 0·4–0·5; glucose, 7·8. Possible changes in the conduction of the nerve impulse, due to the divalent cation concentration falling below 0·7 mM (Frankenhaeuser & Hodgkin, 1957) were avoided by maintaining the external Mg^{2+} concentration,

$[Mg^{2+}]_o$, constant at 2·0 mM. The solution was gassed continuously with 95% O_2 and 5% CO_2; the pH was maintained between 7·2 and 7·5. Neuromuscular synapses were located after bathing the isolated nerve–muscle preparation in 0·1 μM solution of the fluorescent dye, 3-3-diethyl-oxardicarbocyanine iodide ($DiOC_2(5)$) as described previously (Yoshikami & Okun, 1984; Bennett *et al.* 1986; see also Magrassi, Purves & Lichtman, 1987).

Segmental nerves 8 and 9 were taken up in suction glass pipette electrodes. They were stimulated using current pulses of 0·8 ms duration and 6 V amplitude. The stimulation rate was 0·5–1·0 Hz. Intracellular recordings were obtained using microelectrodes filled with 2·0 M-KCl and having resistances of 30–50 MΩ. Extracellular recordings were obtained using microelectrodes filled with 2·0 M-NaCl and having resistances of 20–30 MΩ. Only fibres with resting membrane potentials greater than 60 mV and in which the mean amplitude of miniature end-plate potentials (MEPPs) was greater than 0·5 mV throughout the recording period were studied. Extracellular observations were rejected if they did not meet the following criteria: any shift greater than 20% in the median latency of the first quantum released on each trial; any shift greater than 20% in quantal release rates over three groups of 100 trials; any shift greater than 20% in the mean amplitude of the quanta collected throughout the recording period.

To avoid the effects of electrode pressure on nerve terminals (Fatt & Katz, 1952) the microelectrode was gently placed within 1–3 μm of the visualized terminal branches; the extracellular field potential of the impulse in the nerve terminal was then observed. The electrode was lifted clear of the muscle fibre, repositioned along the terminal branch and gently lowered while looking for end-plate currents (EPCs). The frequency of MEPPs was determined at different times during the period when the electrode was at the recording site. The frequency varied between 0·05 and 0·3 Hz for different release sites. The observations were abandoned if the frequency of MEPPs increased by more than 25% at any recording site during the recording period. Furthermore, the mean quantal content of the EPC ($\bar{m}_e$) was monitored at sites as described by Bennett *et al.* 1986 (see their Fig. 3). This showed that pressure effects caused at most a 10% change in $\bar{m}_e$.

End-plate currents recorded using the focal electrode were collected using an IBM computer and p-clamp software (Axon Instruments) while stimulating either segmental nerve for 200–300 consecutive trials at frequencies of 0·5–1·0 Hz. Amplitude–frequency histograms of end-plate potentials recorded with the intracellular electrode (EPPs) and EPCs were constructed using modifications to the p-clamp software. At least thirty MEPPs were collected and the mean amplitude of these determined. The mean quantal content of the EPP ($\bar{m}$) was determined from the ratio of mean EPP amplitude over 200 trials to mean MEPP amplitude. When about 30% of the impulses failed to evoke transmitter release the method of failures was used to determine $\bar{m}$ (Del Castillo & Katz, 1954). Histograms of the number of quanta released were constructed for the EPCs, and only EPCs which occurred within 5 ms of the negative peak of the presynaptic action potential current were included. Furthermore, only quantal events with amplitudes greater than 1·0 mV were counted, so as to restrict the region of recording to 10–20 μm along a single terminal branch (see Fig. 2 of Bennet *et al.* 1986; also Del Castillo & Katz, 1956; Katz & Miledi, 1965; Bieser, Werning & Zucker, 1984). The mean quantal content of the EPC ($\bar{m}_e$) was determined from the ratio of the total number of quanta released to number of trials. If the average number of quanta released per trial is high, quanta released early can mask quanta which are released later, causing an error in the histogram of numbers of quanta (Katz & Miledi, 1965; Barrett & Stevens, 1972). This would lead to an underestimation of $\bar{m}_e$. This error was minimized by reducing the number of quanta released per trial by decreasing the $[Ca^{2+}]_o$ to 0·4 mM and by maintaining the temperature of the bath at 16 ± 2 °C.

Seventy-two dually innervated muscle fibres were studied with intracellular electrodes but only five of these were suitable for complete study with an extracellular electrode. This was because only these fibres had both terminals accessible on the same surface of the fibre as well as a clear separation from each other. The primary terminal branches along which recordings were made usually begin near the point of nerve entry (see Davey & Bennett, 1982; Bennett, 1983; Bennett, Lavidis & Armson, 1987). This was then taken as the origin of the branch in constructing the secretion profiles given in Figs 1 and 5. The sites of recording along each visualized terminal branch were random with respect to the origin of the branch. This ensured that the peripheral parts of a branch did not have a low $\bar{m}_e$ value caused by terminal damage during recordings made at several sites on the more proximal parts of a branch. Quantal length constants for the decline in $\bar{m}_e$ along terminal branches were determined by a least-squares exponential curve fit to the data in the

equation $\bar{m}_e = \bar{m}_{e,0} \exp(-x/\lambda)$; $\bar{m}_{e,0}$ is the value of $\bar{m}_e$ at the origin of the terminal branch, x is the distance along the branch and λ is the quantal length constant.

The $DiOC_2(5)$-stained fluorescent terminals were photographed at the end of each experiment through a camera attached to the Olympus (BH2) microscope. The muscle was then fixed with 2·5% glutaraldehyde and stained for cholinesterase according to Karnovsky (1964) and photographed. Comparison was then made between the distribution of cholinesterase reaction product, the $DiOC_2(5)$-stained nerve terminal and the positions at which recordings had been made according to their location marked on a transparent overlay placed on the video monitor. The drawings of the terminal branching pattern given in Figs 1 and 5 were derived from those parts of the $DiOC_2(5)$-stained terminal associated with cholinesterase.

RESULTS

Changes in mean quantal content of the EPC along terminal branches of synaptic sites only innervated by nerve 8 or nerve 9

Estimates of the mean quantal content of the EPC were made along the length of eleven terminal branches at eight synaptic sites innervated singly by segmental nerve 8 on the ventral surface of the gluteus muscle; this is termed $\bar{m}_{e,8}$. Each of these terminal branches was separated by more than 10 μm from other terminal branches outside their point of origin and was over 80 μm long (Fig. 1*A*). They therefore fell into the category of medium size (81–120 μm) or long (121–160 μm) branches described by Bennett *et al.* (1986). Two of these branches did not show a consistent decline in $\bar{m}_{e,8}$ which rather remained approximately constant at about 0·2 along the terminal branch. The remaining nine of these branches showed a spatial decline in $\bar{m}_{e,8}$ to which an exponential curve was fitted (Fig. 1*A*). The length constants for these curves (the 'quantal length constant') varied between 26 and 80 μm (52 ± 6 μm, mean ± S.E.M.; Fig. 1*B*). These are similar values to those described for terminal branches of segmental nerve 9 at singly innervated synaptic sites in the mature iliofibularis muscle (Bennett *et al.* 1986).

Estimates of the mean quantal content of the EPC were also made along the length of seven terminal branches at seven synaptic sites innervated singly by segmental nerve 9 on the ventral surface of the gluteus muscle; this is termed $\bar{m}_{e,9}$. These terminal branches fell into either the medium-size or long category; they showed a spatial decline in $\bar{m}_{e,9}$ to which exponential curves were fitted (Fig. 1*C*). No terminal branches in the medium-size or long category failed to show a decline in $\bar{m}_{e,9}$. The quantal length constants for the decline in $\bar{m}_{e,9}$ varied between 26 and 62 μm (40 ± 6 μm; Fig. 1*D*). These are smaller values than those of the nerve 8 terminals, although the difference between the quantal length constants for nerve 8 and nerve 9 was not significant ($P > 0{\cdot}10$).

Changes in mean quantal content of the EPC along terminal branches of synaptic sites dually innervated by nerve 8 and nerve 9

Dual innervation of over 20% of the muscle fibres on the ventral surface accompanies the emergence of a mature topographical map (Malik & Bennett, 1987). At most of these dually innervated sites the quantal content of the EPP for nerve 8 ($\bar{m}_8$) is up to 24 times greater than the quantal content of the EPP for nerve 9 ($\bar{m}_9$; Fig. 2).

The quantal content of the EPP ($\bar{m}$) per 100 μm length of terminal ($(\bar{m} \times 100)$/total

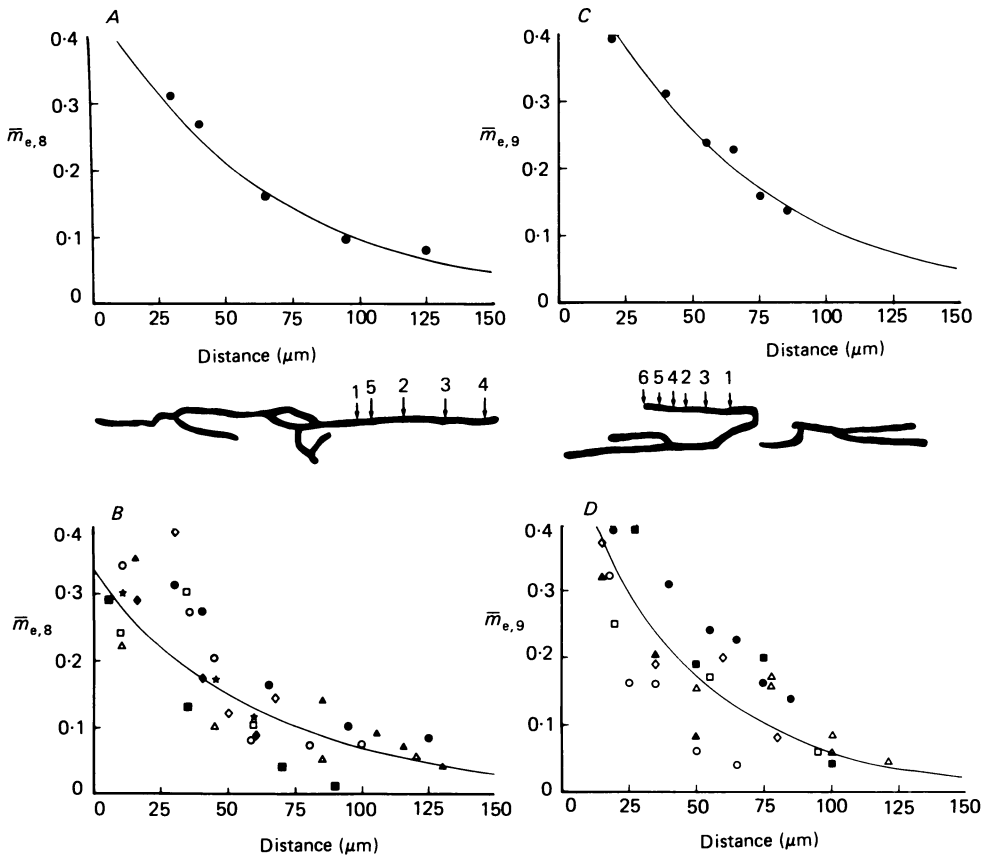

Fig. 1. Changes in $\bar{m}_e$ along the length of terminal branches of nerve 8 or nerve 9 on the surface of the gluteus muscle. *A*, changes in $\bar{m}_e$ along the length of a nerve 8 terminal branch; a drawing is also given of the extent of the nerve terminal, derived from the $DiOC_2(5)$-stained nerve and cholinesterase-stained postsynaptic membrane; the numbers on the terminals give the sequence in which the recordings were made, with arrows indicating the position of the microelectrode; a least-squares exponential curve fit to the data gives a quantal length constant of 67 μm and correlation coefficient of 0·97. *B*, the cumulative results for the changes in $\bar{m}_e$ along the length of medium-size and long nerve 8 terminal branches that showed a decline in $\bar{m}_e$ along their length; a least-squares exponential curve fit to the decline in $\bar{m}_e$ for each terminal in *B* gave the following quantal length constants and correlation coefficients (in parentheses): ■, 26 μm (0·96); □, 59 μm (0·74); ◆, 38 μm (0·99); ▲, 57 μm (0·95); ★, 52 μm (0·98); △, 80 μm (0·80); ◇, 40 μm (0·59); ●, 67 μm (0·97); the quantal length constant for the curve is 59 μm and the correlation coefficient is 0·60. *C*, changes in $\bar{m}_e$ along the length of a nerve 9 terminal branch; a drawing of the extent of the nerve terminal together with the positions of the microelectrode is also given, as in *A*; a least-squares exponential curve fit to the data gives a quantal length constant of 62 μm and correlation coefficient of 0·96. *D*, the cumulative results for the changes in $\bar{m}_e$ along the length of nerve 9 terminal branches; a least-squares exponential curve fit to the value of $\bar{m}_e$ for each terminal gave the following quantal length constants and correlation coefficients (in parentheses): □, 47 μm (0·99); △, 46 μm (0·80); ●, 62 μm (0·96); ▲, 26 μm (0·93); ○, 27 μm (0·93); ■, 34 μm (0·84); ◇, 51 μm (0·84); the length constant for the curve is 47 μm and the correlation coefficient is 0·70. The $[Ca^{2+}]_o$ varied between 0·35 and 0·40 mM.

terminal length) was determined for synaptic sites singly innervated by nerve 8 or nerve 9 as well as for sites dually innervated by both nerves during this period of development. Both $\bar{m}_8$ and $\bar{m}_9$ declined per 100 μm length of terminal as the total length of terminals increased at singly innervated synaptic sites (Fig. 3*A* and *B*). In both cases this decline was approximately exponential, with a length constant of

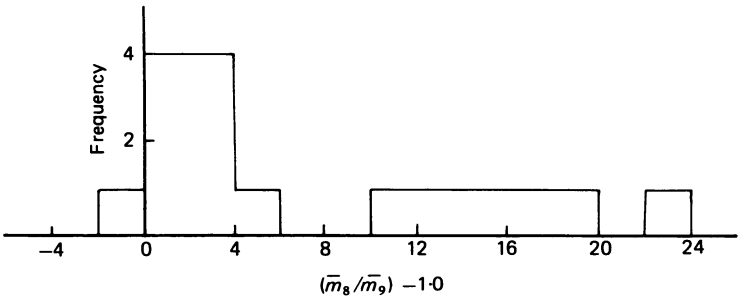

Fig. 2. The dominance of segmental nerve 8 terminals at synaptic sites dually innervated by both nerve 8 and nerve 9 on the ventral surface of the developing gluteus muscle. Frequency distribution of $(\bar{m}_{e,8}/\bar{m}_{e,9}-1{\cdot}0)$ for dually innervated sites. Note that $\bar{m}_8 > \bar{m}_9$ in all but one case.

400 μm. At dually innervated sites $\bar{m}_8$ per 100 μm length of terminal fell close to (but generally below) the average curve for $\bar{m}_8$ per 100 μm at singly innervated sites (compare Fig. 3*C* with 3*B*). These nerve 8 terminals were in the same total terminal length size range of up to about 650 μm as nerve 8 terminals on singly innervated fibres. In contrast, the largest nerve 9 terminals were substantially smaller at dually innervated synaptic sites (a maximum of 250 μm total terminal length compared with up to 650 μm on singly innervated fibres; see Fig. 3*A* and *C*). The $\bar{m}_9$ per 100 μm length of terminal at dually innervated sites was very small for all terminals compared with that at singly innervated sites (compare Fig. 3*C* with 3*A*). These observations indicate that the relatively low quantal secretion from nerve 9 terminals at dually innervated sites is not due to their small size alone. Nerve 9 terminals at dually innervated sites therefore provide an opportunity to examine changes in $\bar{m}_e$ along the terminal branches of suppressed nerve terminals.

Estimates of both $\bar{m}_{e,8}$ and $\bar{m}_{e,9}$ were made along the length of medium-size or long terminal branches at five dually innervated synaptic sites (Fig. 4). Seven of the nine terminal branches of nerve 8 showed a spatial decline in $\bar{m}_{e,8}$ to which exponential curves were fitted (Fig. 5*A* and *B*). The quantal length constants for these branches varied between 29 and 43 μm (35 $\pm$ 3 μm; Fig. 6*C*). The mean length constants for $\bar{m}_{e,8}$ decline at these dually innervated sites is smaller than that for $\bar{m}_{e,8}$ decline at singly innervated sites, and this was significant ($P < 0{\cdot}05$). However, it should be noted that the average length of terminal branches analysed at singly innervated nerve 8 sites was 103 $\pm$ 7 μm, whereas that of nerve 8 at dually innervated sites was 83 $\pm$ 3 μm. It may be that the shorter terminal branches have somewhat shorter length constants for the spatial decay of $\bar{m}_e$ (for terminals 80 $\pm$ 5 μm long the average length constant was 35 $\pm$ 3 μm ($n = 8$) and for terminals 125 $\pm$ 5 μm long it was 57 $\pm$ 8 μm ($n = 5$)). Two of the nine terminal branches of nerve 8 did not show a

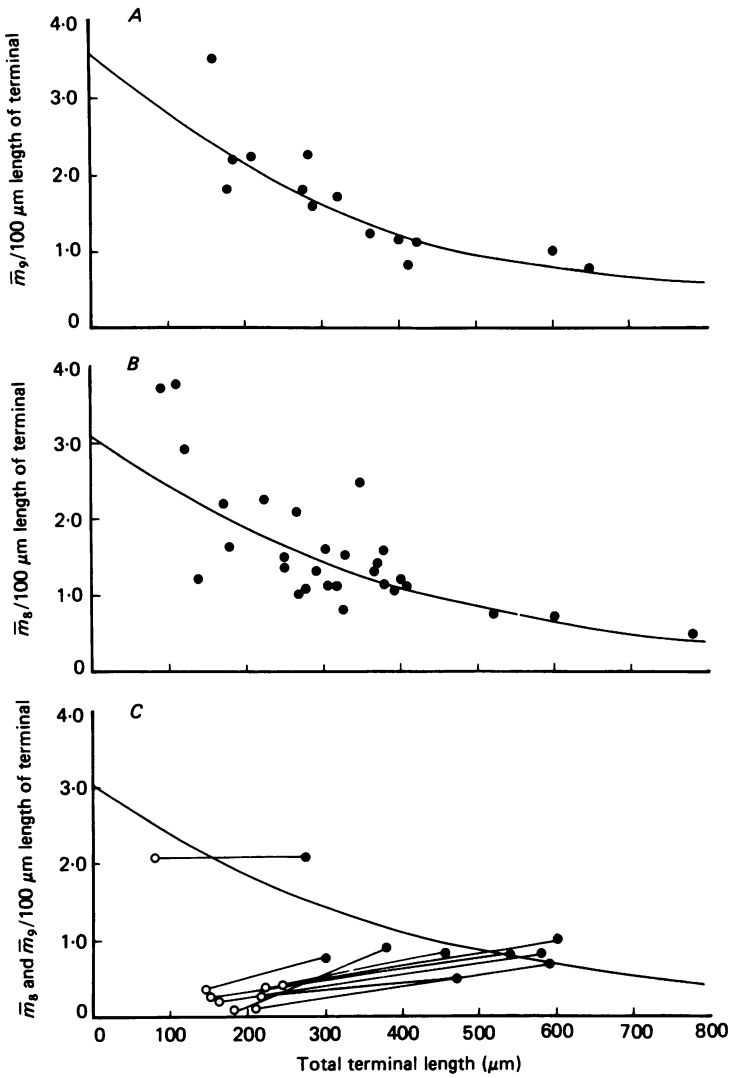

Fig. 3. Changes in quantal content of the intracellularly recorded EPP ($\bar{m}$) per 100 μm length of terminal branch for terminals of different total length at singly and dually innervated synaptic sites. *A*, the decline in $\bar{m}/100$ μm terminal length of nerve 9 as the total terminal length increases ($n = 14$ terminals on singly innervated fibres in the ventral surface of the gluteus muscle); the least-squares exponential curve fit gives a length constant of 400 μm with correlation coefficient 0·74. *B*, the decline in $\bar{m}/100$ μm terminal length of nerve 8 as the total terminal length increases ($n = 29$ terminals on singly innervated fibres on the ventral surface of the gluteus muscle); the least-squares exponential curve fit gives a length constant of 400 μm, with correlation coefficient 0·60. *C*, comparison between the $\bar{m}/100$ μm terminal length of nerve 8 (●) and nerve 9 (○) for dually innervated fibres; each pair of values is joined by a line. The curve is the same as that in *B*. Note that at these dually innervated synaptic sites $\bar{m}_9/100$ μm is generally less than half that of $\bar{m}_8/100$ μm.

decline in $\bar{m}_{e,8}$ (Fig. 6*B*); this is a similar proportion to that found at singly innervated sites. None of the five terminal branches of nerve 9 showed a spatial decline in $\bar{m}_{e,9}$; rather, $\bar{m}_{e,9}$ remained fairly constant and low along the length of the branches (Fig. 6*A*). Thus all the terminal branches of nerve 9 at dually innervated sites showed depressed values of $\bar{m}_{e,9}$ and these did not decline along the length of branches (Fig. 6), whereas all seven terminal branches of nerve 9 at singly innervated sites showed a decline in $\bar{m}_{e,9}$ from an initially large value (Fig. 1*D*).

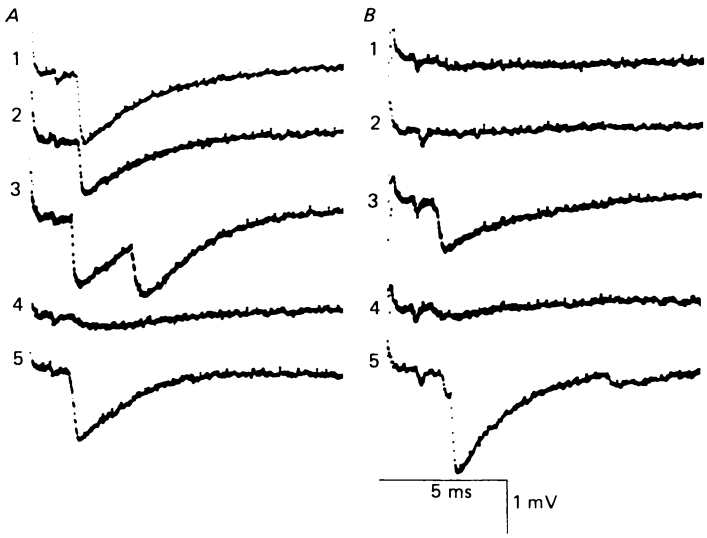

Fig. 4. Focal extracellular recordings of quantal events at the beginnings of terminal branches of nerve 8 (*A*) and nerve 9 (*B*) at a dually innervated synaptic site. Successive traces give the responses to successive stimuli (1–5) applied to the motor nerve at 1 Hz (stimuli of 0·8 ms duration and 6 V strength). AC coupling used in all records. $[Ca^{2+}]_o$ is 0·35 mM.

DISCUSSION

The mean quantal content of the EPP at dually innervated synaptic sites

In amphibian muscle there is an inverse relationship beween the level of quantal secretion per unit length of nerve terminal and the total length of the terminal (Nudell & Grinnell, 1982). This was confirmed in the present work for sites innervated by nerve 8 or nerve 9. However, nerve 9 terminals at dually innervated sites secreted very few quanta per unit length of terminal compared with nerve 8 terminals, indicating the suppression of quantal secretion at nerve 9 terminals. Although it has been reported that synaptic efficacy is low at polyneuronally innervated sites compared with mononeuronally innervated sites (Haimann, Mallart, Ferre & Zilber-Gachelin, 1981; Trussell & Grinnell, 1985), only nerve 9 terminals showed low efficacy at dually innervated sites on the ventral surface of the gluteus muscle during the long period of refinement of the topographical map in these toad muscles (Malik & Bennett, 1987). This is in contrast to the synaptic efficacies of both terminals at dually innervated synaptic sites in mature frog muscle (Herrera, 1984), which are usually the same (Werle & Herrera, 1987).

The mean quantal content of the EPC along terminal branches at synaptic sites dually innervated by nerve 8 or nerve 9

At dually innervated sites nearly all nerve 8 terminal branches showed an approximately exponential decline in $\bar{m}_e$. By contrast, the quantal release per unit length of terminal was very low for nerve 9 terminal branches at dually innervated

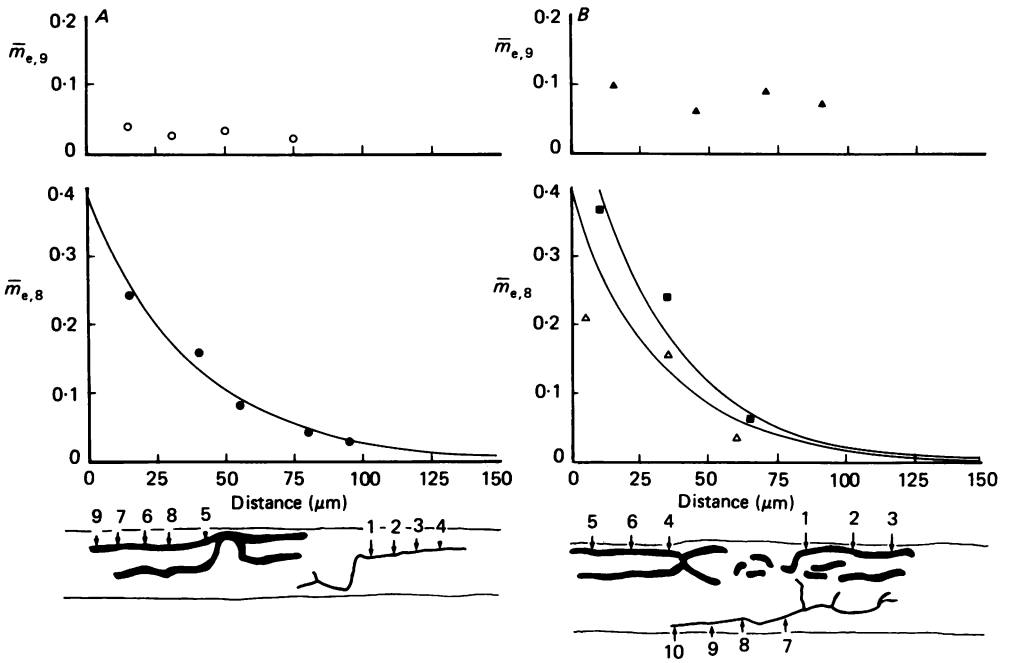

Fig. 5. Changes in $\bar{m}_e$ along the length of terminal branches of nerves 8 and 9 ($\bar{m}_{e,8}$ and $\bar{m}_{e,9}$) on two different (*A* and *B*) dually innervated fibres on the ventral surface of the gluteus muscle. In each case a drawing of the extent of the nerve terminal is given, derived from the $DiOC_2(5)$-stained nerve and terminal cholinesterase-stained postsynaptic membrane (thick branches are nerve 8 and thin nerve 9). The numbers on the terminals give the sequence in which the recordings were made; arrows indicate the position of the microelectrode. Least-squares exponential curve fits to the data for $\bar{m}_{e,8}$ in *A* gives a quantal length constant and correlation coefficient (in parentheses) of 36 μm (0·98). Least-squares exponential curve fits to the two sets of data for $\bar{m}_{e,8}$ in *B*, corresponding to the measurements on two branches, give quantal length constants of 30 μm (■; correlation coefficient 0·94) and 29 μm (△; correlation coefficient 0·84). Note that $\bar{m}_{e,9}$ is uniformly low for both nerve 9 terminal branches in *A* and *B*.

sites: the proximal release sites had secreted small numbers of quanta like the distal release sites. Similar results have possibly been observed by D'Alonzo & Grinnell (1985) who comment that 'some junctions had large regions of terminal that released very little transmitter. These also showed multiple myelinated axonal inputs, and may have been polyneuronally innervated junctions in which one of the inputs was weaker than the others.'

The physical basis for the changes in the probability of secretion at different release sites along terminal branches at either mononeuronally or polyneuronally

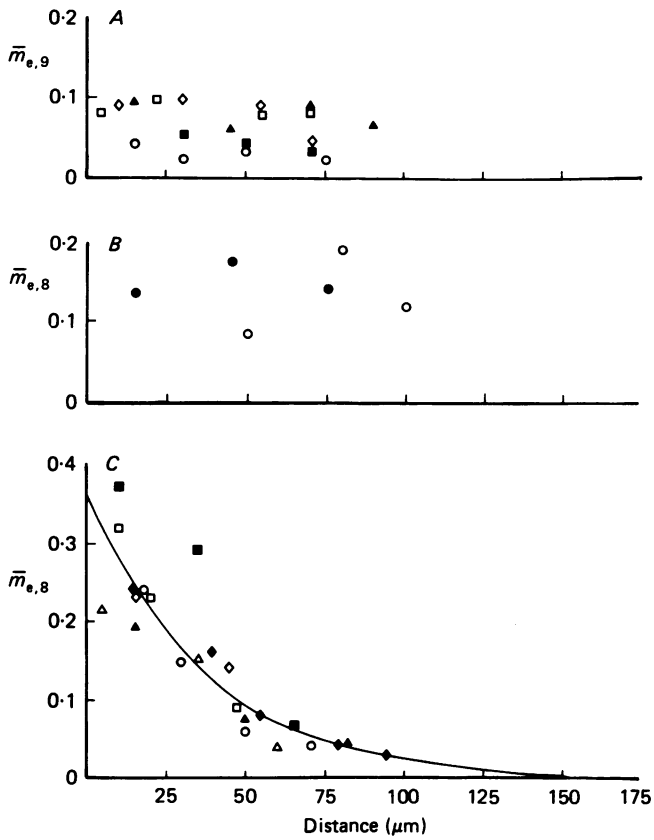

Fig. 6. Cumulative results for the changes in $\bar{m}_e$ along the length of nerve 8 terminal branches ($\bar{m}_{e,8}$) and nerve 9 terminal branches ($\bar{m}_{e,9}$) at five dually innervated synaptic sites on the ventral surface of the gluteus muscle. *A* gives the results for all nerve 9 branches studied; *B* gives the results for those nerve 8 branches that did not show a decline in $\bar{m}_{e,8}$ from an initially high value; *C* gives the results for those nerve 8 branches that did show a decline in $\bar{m}_{e,8}$ from an initially high value. A least-squares exponential curve fit to the decline in $\bar{m}_e$ for each nerve 8 terminal ($\bar{m}_{e,8}$) in *C* gave the following quantal length constants and correlation coefficients (in parentheses): ◇, 48 μm (0·98); ▲, 42 μm (0·99); ◆, 36 μm (0·98); ○, 29 μm (0·98); ■, 30 μm (0·94); △, 29 μm (0·81); ▲, 43 μm (0·99). The quantal length constant and correlation coefficient (in parentheses) for the curve is 36 μm (0·89). The $[Ca^{2+}]_o$ varied between 0·35 and 0·40 mM. Note that although the estimates of $\bar{m}_{e,9}$ for some branches in *A* do not extend up to 80 μm from the point of branch origin, all these branches were greater than 80 μm long (see for example Fig. 5*A*).

innervated sites has not been determined. One possibility is that intramembranous particles at the active zone which may be Ca^{2+} channels decrease in density at release sites with low secretion probabilities (Heuser, Reese & Landis, 1974; Llinas, 1982; Pawson & Grinnell, 1984; Herrera, Grinnell & Wolowske, 1985*a*). In multiply innervated end-plates, for example, terminals with organized active zones showed vesicle openings while terminals in the same synaptic gutter with disorganized active zones showed no vesicle openings (Ko, 1984, 1985). It is possible that Ca^{2+} influx is lower at release sites with a low probability for secretion because of either relatively short or disorganized active zones.

The lengths of active zones exposed to postsynaptic folds in the terminal gutter have been measured along terminal branches in the iliofibularis muscle (Davey & Bennett, 1982; Bennett *et al.* 1987). Terminal branches longer than about 80 μm showed a decline in the length of the exposed active zone from proximal parts of the terminal to distal parts. This is consistent with the idea that the organization of active zone particles influences the probability of quantal secretion. The length of active zone exposed to the postsynaptic folds may be determined by the extent to which Schwann cells intercalate their processes between the active zone and the postsynaptic folds (Herrera, Grinnell & Wolowske, 1985*b*; see Figs 2 and 6 of Bennett *et al.* 1987). If this is the case, then the uniformly low value of $\bar{m}_e$ along terminal branches of nerve 9 at dually innervated sites may be due to Schwann cells masking the active zones from the postsynaptic folds at both proximal and distal sites. It will be interesting to compare the ultrastructure of active zones and their relationship to Schwann cells at nerve 8 and nerve 9 terminals on dually innervated synaptic sites in the immature muscle.

We are most grateful to Dr S. Redman for his comments on the manuscript. N. A. Lavidis was supported by an NHMRC Post-doctoral Fellowship.

REFERENCES

BARRETT, E. F. & STEVENS, C. F. (1972). Quantal independence and uniformity of presynaptic release kinetics at the frog neuromuscular junction. *Journal of Physiology* **227**, 665–689.

BENNETT, M. R. (1983). Development of neuromuscular synapses. *Physiological Reviews* **63**, 915–1049.

BENNETT, M. R., JONES, P. & LAVIDIS, N. A. (1986). The probability of quantal secretion along visualized terminal branches at amphibian (*Bufo marinus*) neuromuscular synapses. *Journal of Physiology* **379**, 257–274.

BENNETT, M. R. & LAVIDIS, N. A. (1979). The effect of Ca ions on the secretion of quanta evoked by an impulse at nerve terminal release sites. *Journal of General Physiology* **74**, 429–456.

BENNETT, M. R. & LAVIDIS, N. A. (1982*a*). Development of the topographical projection of motoneurones to amphibian muscle accompanies motoneurone death. *Developmental Brain Research* **2**, 448–452.

BENNETT, M. R. & LAVIDIS, N. A. (1982*b*). Variation in quantal secretion at different release sites along developing and mature motor terminal branches. *Developmental Brain Research* **5**, 1–9.

BENNETT, M. R. & LAVIDIS, N. A. (1986). Topographical projections of segmental nerves to the frog glutaeus muscle during loss of polyneuronal innervation. *Journal of Physiology* **375**, 303–325.

BENNETT, M. R., LAVIDIS, N. A. & ARMSON, F. M. (1987). Changes in the dimensions of release sites along terminal branches at amphibian neuromuscular synapses. *Journal of Neurocytology* **16**, 221–237.

BENNETT, M. R. & PETTIGREW, A. (1975). The formation of synapses in amphibian striated muscle during develoment. *Journal of Physiology* **252**, 203–239.

BIESER, A., WERNIG, A. & ZUCKER, H. (1984). Different quantal responses within single frog neuromuscular junctions. *Journal of Physiology* **350**, 401–412.

COUTEAUX, R. & PECOT-DECHAVASSINE, M. (1968). Vesicules synaptiques et poches au niveau de les 'zones actives' de la junction neuromusculaire. *Comptes rendus hebdomadaires des séances de l'Académie des sciences* **271**, 2346–2349.

D'ALONZO, A. J. & GRINNELL, A. D. (1985). Profiles of evoked release along the length of frog motor nerve terminals. *Journal of Physiology* **359**, 235–258.

DAVEY, D. F. & BENNETT, M. R. (1982). Variation in the size of synaptic contacts along developing and mature motor terminal branches. *Developmental Brain Research* **5**, 11–22.

DEL CASTILLO, J. & KATZ, B. (1954). Quantal components of the end-plate potential. *Journal of Physiology* **124**, 560–573.

DEL CASTILLO, J. & KATZ, B. (1956). Localization of active spots within the neuromuscular junction of the frog. *Journal of Physiology* **132**, 630–649.

DREYER, F., PEPER, K. M., AKERT, D. M., SANDRI, C. & MOORE, H. (1973). Ultrastructure of the 'active zone' in the frog neuromuscular junction. *Brain Research* **62**, 373–380.

FATT, P. & KATZ, B. (1952). Spontaneous subthreshold activity at motor nerve endings. *Journal of Physiology* **117**, 109–128.

FRANKENHAEUSER, B. & HODGKIN, A. L. (1957). The action of calcium on the electrical properties of squid axons. *Journal of Physiology* **137**, 218–244.

HAIMANN, C., MALLART, A., TOMAS, I., FERRE, J. & ZILBER-GACHELIN, N. F. (1981). Interactions between motor axons from two different nerves reinnervating the pectoral muscle of *Xenopus laevis*. *Journal of Physiology* **310**, 257–272.

HERRERA, A. A. (1984). Polyneuronal innervation and quantal transmitter release in formamide-treated frog sartorius muscles. *Journal of Physiology* **355**, 267–280.

HERRERA, A. A., GRINNELL, A. D. & WOLOWSKE, B. (1985*a*). Ultrastructural correlates of naturally occurring differences in transmitter release efficacy in frog motor nerve terminals. *Journal of Neurocytology* **14**, 193–202.22.

HERRERA, A. A., GRINNELL, A. D. & WOLOWSKE, B. (1985*b*). Ultrastructural correlates of experimentally altered transmitter release efficacy in frog motor nerve terminals. *Neuroscience Letters* **16**, 491–500.

HEUSER, J. E., REESE, T. S. & LANDIS, D. M. (1974). Functional changes in frog neuromuscular junction studies with freeze-fracture. *Journal of Neurocytology* **3**, 108–131.

KARNOVSKY, M. J. (1964). The localization of cholinesterase activity in rat cardiac muscle by electron microscopy. *Journal of Cell Biology* **23**, 217–232.

KATZ, B. & MILEDI, R. (1965). The measurement of synaptic delay, and the time course of acetylcholine release at the neuromuscular junction. *Proceedings of the Royal Society* B **161**, 483–495.

KO, C. P. (1984). Regeneration of the active zone at the frog neuromuscular junction. *Journal of Cell Biology* **98**, 1685–1695.

KO, C. P. (1985). Regeneration of the active zone at the developing neuromuscular junctions in larval and adult bullfrogs. *Journal of Neurocytology* **14**, 487–512.

LETINSKY, M. R. & MORRISON-GRAHAM, K. (1980). Structure of developing frog neuromuscular functions. *Journal of Neurocytology* **9**, 321–342.

LLINAS, R. R. (1982). Calcium in synaptic transmission. *Scientific American* **247**, 56–65.

MAGRASSI, L., PURVES, D. & LICHTMAN, J. W. (1987). Fluorescent probes that stain living nerve terminals. *Journal of Neuroscience* **7**, 1207–1214.

MALIK, M. & BENNETT, M. R. (1987). Loss of polyneuronal innervation and establishment of a topographical map in the glutaeus muscle of *Bufo marinus* during generation of secondary muscle cells. *Developmental Brain Research* **34**, 173–189.

MCMAHAN, U. J., SPITZER, N. L. & PEPER, K. (1972). Visual identification of nerve terminals in living isolated skeletal muscle. *Proceedings of the Royal Society* B **181**, 421–430.

MILLER, T. M. & HEUSER, J. E. (1984). Endocytosis of synaptic vesicle membrane at the frog neuromuscular junction. *Journal of Cell Biology* **98**, 685–698.

MORRISON-GRAHAM, K. (1983). An anatomical and electrophysiology study of synapse elimination at the developing frog neuromuscular junction. *Developmental Biology* **890**, 298–311.

NUDELL, B. M. & GRINNELL, A. D. (1982). Inverse relationship between transmitter release and terminal length in synapses on frog muscle fibers of uniform input resistance. *Journal of Neuroscience* **2**, 216–224.

PAWSON, P. A. & GRINNELL, A. D. (1984). Post-tetanic potentiation in strong and weak neuromuscular junctions: physiological differences caused by a differential calcium influx. *Brain Research* **323**, 311–315.25.

ROBITAILLE, R. & TREMBLAY, J. P. (1987). Non-uniform release at the frog neuromuscular junction: evidence of morphological and physiological plasticity. *Brain Research Reviews* **12**, 95–116.

SHERRINGTON, C. S. (1892). Notes on the arrangement of some motor fibres in the lumbo-sacral plexus. *Journal of Physiology* **13**, 621–772.

TRUSSELL, L. D. & GRINNELL, A. D. (1985). The regulation of synaptic strength within motor units of the frog cutaneous pectoris muscle. *Journal of Neuroscience* **1**, 243–254.

WERLE, M. J. & HERRERA, A. A. (1987). Synaptic competition and the persistence of polyneuronal innervation at frog neuromuscular junctions. *Journal of Neurobiology* **18**, 375–389.

YOSHIKAMI, D. & OKUN, L. M. (1984). Staining of living presynaptic nerve terminals with selective fluorescent dyes. *Nature* **310**, 53–56.

ZEFIROV, A. L. & STOLOV, E. L. (1981). A model of mediator secretion in the neuromuscular synapse based on spatial heterogeneity of acetylcholine quantum release probability. *Neirofiziologiya* **14**, 233–240.